

Numerical test of approximate single-step propagators: Harmonic power series expansions versus system-specific split operator representations

Alexander N. Drozdov* and Shigeo Hayashi

Department of Applied Physics and Chemistry, University of Electro-Communications, 1-5-1 Chofugaoka, Chofu, Tokyo 182-8585, Japan

(Received 9 September 1998)

This paper compares the efficiency and accuracy of different second-order approximations for the single-step propagator obtained by means of the power series expansion formalism and the split operator method. The former is based on a harmonic reference system, while the latter allows for the use of physically motivated (anharmonic) zeroth-order representations. Three typical examples—a system-bath Hamiltonian, a Hénon-Heiles anharmonic resonating system, and a Fokker-Planck chaotic model—are considered in the present testing. The examples cover a variety of situations with strongly anharmonic coupling. Although no system-specific reference system is involved in the power series representation of the propagator, it quite accurately describes the dynamics of very anharmonic processes in the *entire* time domain even though the coupling is *strong*. Another appealing feature of the approach is that it is essentially *analytical* and therefore *does not* require any computational effort to implement. This makes the power series expansion technique particularly attractive for efficiently treating many-body problems. In contrast, numerical implementation of the split operator method can be arduous as a general multidimensional calculation, while its utility is in general restricted to the separable limit, when the coupling is almost turned off. In that limit the method indeed provides accurate results over a broad range of t . With increasing coupling, however, the efficiency of the method deteriorates very rapidly regardless of the particular choice of the zeroth-order representation. [S1063-651X(99)08601-8]

PACS number(s): 05.40.-a, 02.50.Ey

I. INTRODUCTION

Feynman path integration [1] has, in recent years, been the subject of intense study, and it has been found to be extremely promising as an approach to multidimensional problems of quantum and statistical mechanics [2,3]. Particularly exciting is the fact that the dynamics of fully quantal many-body problems can be interpreted in terms of classical (Feynman's) paths that are one-dimensional lines regardless of the number of degrees of freedom involved. Numerical evaluation of the path integral requires discretization of the paths via time slicing. Since long time evolution is achieved by repeated application of the evolution operator, one may employ approximations of the evolution operator suitable only for short time propagation. This results in a multidimensional integral. Clearly, the convergence of path integral calculations depends critically on how good the approximation for the short time evolution operator is. The better the short time propagator, the longer the time step one can employ. The standard procedure of approximating the evolution operator for short time employs the symmetric Trotter breakup based on partitioning the Hamiltonian into potential and kinetic energy terms [4]. This splitting is exact for any time in the limit of free-particle motion. Otherwise, it requires very short time increments for accuracy. Consequently, the dimension of the resulting path integral can be very high if the desired propagation time and/or the dimensionality of the system are large. The only possible way to evaluate it is to

employ Monte Carlo techniques [5]. A number of impressive calculations of the low-temperature properties of quantum many-body systems have been performed using Monte Carlo path integration [6]. The latter, however, suffers from statistical errors. Yet another difficulty lies in the inefficiency of statistical Monte Carlo sampling techniques when used to integrate highly oscillatory functions which occur due to the oscillatory nature of the quantum time evolution operator.

Several methods have been proposed to improve Monte Carlo techniques [7]. Significant advances have also been made in the development of higher-order approximations to the short time propagator valid for longer time [8–14]. An extensive study of their relative efficacy can be found in a previous paper [15]. Although some of these methods have improved the statistics of path integral calculations allowing time steps one order of magnitude larger than these possible with the standard Trotter splitting [13,14], their range of validity is in most nontrivial cases too short to allow an accurate numerical evaluation of the path integral for long times. Thus, in spite of the above advances, the quantum and statistical mechanics of truly multidimensional systems remains beyond the computational powers of even the fastest path integral algorithms.

An important exception involves problems where an arbitrary one-dimensional system is linearly coupled to a harmonic bath. Makri and co-workers [16] suggested a path integral method to deal very efficiently with such situations. The starting point is an improved quasiadiabatic propagator based on an adiabatic partitioning of the Hamiltonian. The propagator is evaluated numerically in terms of the Trotter product formula and a basis set method. The approach is particularly attractive for two reasons. First, the harmonic bath appears in the path integral expression as a Gaussian

*Permanent address: Institute for High Temperatures, 13/19 Izhorskaya Street, 127412 Moscow, Russia.

integral. The latter is easily integrated out *analytically*, giving rise to a nonlocal influence functional and reducing the problem to a path integral for the system coordinate only. Second, the quasiadiabatic propagator is exact not only in the separable limit but also for a strongly coupled Hamiltonian if the bath is fast. In both limits this leads to a reasonable description of the dynamics with fewer time slices, allowing an evaluation of the path integral by quadratures. The resulting methodology does not employ Monte Carlo procedures and thus yields numerically exact results free of statistical noise. More recently the approach was extended to a system coupled to a set of *anharmonic* noninteracting degrees of freedom [17]. Although the path integral method has appeared to be rather complicated for numerical implementation, Makri and co-workers managed to apply it successfully to a number of system-bath models. In addition, these authors claimed that once their quasiadiabatic representation is exact for *any* time in the separable limit, it may be used as a *single step propagator* for fairly long times with moderate coupling strengths. The issue of whether the quasiadiabatic approximation for the propagator preserves its significance for moderate coupling will be addressed in Sec. III of this paper.

Yet another exception is the work of Drozdov [18,19], who elaborated a theory that combines the sum acceleration technique, as well as the power series expansion method of Makri and Miller [8]. The basic ideas are representing the full propagator as a product of the harmonic-oscillator propagator with the configuration function, and expanding the exponent of the configuration function in a power series in a given function of t . The approach distinguishes itself from other methods in that it gives global approximations valid not only for short times, but also in intermediate and long time domains. In many practical applications the expansion coefficients can be evaluated *analytically* for any number of degrees of freedom involved. This makes the power series expansion method particularly attractive for treating many-body problems. However, the utility of the method has been illustrated only on one-dimensional models.

It is our aim here to compare the relative efficacy of the two approaches in giving precise approximations to the single-step propagator valid for the entire time domain. To this end, we consider three typical two-dimensional models that cover a variety of physically meaningful situations with strongly anharmonic mode coupling. The models selected have been frequently used by many researchers as benchmarks of different numerical methods and therefore should present a challenge for the considered perturbation techniques. The remainder of the paper is organized as follows. In Sec. II we review the split operator method and the power series expansion formalism, and discuss the numerical techniques that we used. In Sec. III the applications are presented. Finally, Sec. IV summarizes our conclusions.

II. THEORY

In this paper we deal with the propagator of the partial differential equation of a generic type given by (summation rule over repeated indices is always implied)

$$\begin{aligned}\partial_t P(\mathbf{x}, t | \mathbf{x}^0) &= LP(\mathbf{x}, t | \mathbf{x}^0) \\ &\equiv [\tfrac{1}{2} D_{ij} \partial_{ij}^2 - \partial_i G_i(\mathbf{x}) - \Phi(\mathbf{x})] P(\mathbf{x}, t | \mathbf{x}^0),\end{aligned}\quad (2.1)$$

where $\mathbf{x} = (x_1, \dots, x_n)$, and L stands for the time-independent Cartesian Fokker-Planck operator defined by Eq. (2.1). We assume that the drift vector $\mathbf{G}(\mathbf{x})$ and the diffusion matrix \mathbf{D} entering this operator obey potential conditions [20], so that for $\Phi(\mathbf{x}) = 0$ the logarithm of the stationary solution of the above equation can be obtained by simple integration,

$$U(\mathbf{x}) = -2 \int^{\mathbf{x}} d\mathbf{q} \cdot \mathbf{D}^{-1} \mathbf{G}(\mathbf{q}), \quad (2.2)$$

to give

$$P_{\text{st}}(\mathbf{x}) \equiv P(\mathbf{x}, t \rightarrow \infty | \mathbf{x}^0) = N^{-1} \exp[-U(\mathbf{x})], \quad (2.3)$$

with a normalization constant N defined by Eq. (2.34). Using the standard transformation

$$P(\mathbf{x}, t | \mathbf{x}^0) = \sqrt{P_{\text{st}}(\mathbf{x})/P_{\text{st}}(\mathbf{x}^0)} \psi(\mathbf{x}, t | \mathbf{x}^0), \quad (2.4)$$

one finds that the dynamics described by Eq. (2.1) is also governed by a Schrödinger-type equation

$$-\partial_t \psi(\mathbf{x}, t | \mathbf{x}^0) = H \psi(\mathbf{x}, t | \mathbf{x}^0) \equiv [-\tfrac{1}{2} D_{ij} \partial_{ij}^2 + V(\mathbf{x})] \psi(\mathbf{x}, t | \mathbf{x}^0), \quad (2.5)$$

where H denotes the Hamiltonian operator with the transformed potential

$$V(\mathbf{x}) = \Phi(\mathbf{x}) + \tfrac{1}{2} (\partial_i G_i + D^{ij} G_i G_j). \quad (2.6)$$

Hereby D^{ij} means the element of the inverse matrix \mathbf{D}^{-1} . Finally, we note that besides the propagator itself, the quantity of interest is also the probability distribution

$$P(\mathbf{x}, t) = \psi(\mathbf{x}, t | \mathbf{x}) / \text{Tr}[e^{-tH}]. \quad (2.7)$$

It is not difficult to show that with t going to infinity, this function reduces to the square of the ground state solution $\psi_0(\mathbf{x})$ of the Hamiltonian (2.5),

$$P(\mathbf{x}, t \rightarrow \infty) = \psi_0^2(\mathbf{x}). \quad (2.8)$$

A. Split operator method

The basic idea of the method is to split the Hamiltonian operator into a reference part H_r and a disturbance H_d , reading

$$H = H_r + H_d, \quad (2.9)$$

and then to employ a decomposition of the time evolution operator valid to a given order in the time increment t . In the present paper we restrict our consideration to the simplest and most commonly used breakup, the so called symmetric Trotter product formula

$$e^{-t(H_r + H_d)} = e^{-tH_d/2} e^{-tH_r} e^{-tH_d/2} + O(t^3). \quad (2.10)$$

The breakup is exact for any t if and only if the commutator of H_r and H_d commutes with both H_r and H_d . Nevertheless, throughout, Eq. (2.10) preserves its significance as a convenient starting point for constructing long time approximations provided the reference operator is chosen such that $[H, [H_r, H_d]]$ is small. As noted in Sec. I, the standard short time propagator is obtained in terms of Eq. (2.10) by splitting the Hamiltonian into potential and kinetic energy terms

$$H_r = -\frac{1}{2}D_{ij}\partial_{ij}^2, \quad H_d = V(\mathbf{x}). \quad (2.11)$$

This leads to a second-order free-particle coordinate representation of the form

$$\begin{aligned} \psi_{fp}(\mathbf{x}, t | \mathbf{x}^0) &= [(2\pi t)^n \det \mathbf{D}]^{-1/2} \\ &\times \exp\left\{-\frac{1}{2t}(\mathbf{x} - \mathbf{x}^0) \cdot \mathbf{D}^{-1}(\mathbf{x} - \mathbf{x}^0) \right. \\ &\left. - \frac{t}{2}[V(\mathbf{x}) + V(\mathbf{x}^0)]\right\}. \end{aligned} \quad (2.12)$$

One can readily show that the commutator neglected in deriving Eq. (2.12) is proportional to [14]

$$t^3 D_{ij}(\partial_i V)(\partial_j V).$$

This neglect is quite severe, and introduces a large error that has to be compensated for by a very small time increment t .

An obvious way to refine the Trotter breakup is to employ an improved zeroth-order representation of the propagator that is accurate for a particular problem, but much better behaved than the free-particle basis $\exp(-\frac{1}{2}tD_{ij}\partial_{ij}^2)$. For example, choosing H_r as the separable part of the Hamiltonian and H_d as a potential term which mixes the degrees of freedom [21],

$$H_r = -\frac{1}{2}D_{ii}\partial_{ii}^2 + V_i(x_i) = \sum_{i=1}^n H_i, \quad H_d = F(\mathbf{x}), \quad (2.13)$$

yields the following system-specific approximation:

$$\psi_{sa}(\mathbf{x}, t | \mathbf{x}^0) = \langle \mathbf{x} | e^{-tH_r} | \mathbf{x}^0 \rangle \exp\left\{-\frac{1}{2}t[F(\mathbf{x}) + F(\mathbf{x}^0)]\right\}. \quad (2.14)$$

The best zeroth-order propagators cannot be expressed in closed form in general, and must therefore be computed *numerically*. This can be done rather efficiently by standard one-dimensional grid or basis set methods because H_r is chosen to be separable:

$$\langle \mathbf{x} | e^{-tH_r} | \mathbf{x}^0 \rangle = \prod_{i=1}^n \langle x_i | e^{-tH_i} | x_i^0 \rangle. \quad (2.15)$$

The scheme based on Eq. (2.14) will be referred to as the *separable approximation* (SA). The approach is applicable to any Hamiltonian with a diagonal diffusion matrix, whose potential can be split according to Eq. (2.13).

Another important situation, often met in real physical processes, involves problems which can be represented with a so called system-bath approximation. The latter usually

involves a relevant degree of freedom x (the system) coupled to a set of *noninteracting* degrees of freedom y_i (the bath):

$$H = -\frac{1}{2}D_x\partial_{xx}^2 + V(x) - \frac{1}{2}D_{ii}\partial_{ii}^2 + V_i(x, y_i). \quad (2.16)$$

Then splitting the full Hamiltonian into the one-dimensional reference (describing the system of interest) and the rest

$$H_r = -\frac{1}{2}D_x\partial_{xx}^2 + V(x), \quad (2.17)$$

$$H_d = -\frac{1}{2}D_{ii}\partial_{ii}^2 + V_i(x, y_i) = \sum_{i=1}^n H_i,$$

we arrive with Eq. (2.10) at the following *quasiadiabatic approximation* (QA) for the propagator:

$$\begin{aligned} \psi_{qa}(x, \mathbf{y}, t | x_0, \mathbf{y}^0) &= \langle x | e^{-tH_r} | x_0 \rangle \int d\mathbf{z} \langle \mathbf{y} | e^{-tH_d(x)/2} | \mathbf{z} \rangle \\ &\times \langle \mathbf{z} | e^{-tH_d(x_0)/2} | \mathbf{y}^0 \rangle. \end{aligned} \quad (2.18)$$

The scheme is applicable to an arbitrary two-dimensional problem governed by a general potential, as well as to multidimensional Hamiltonians allowing adiabatic separation of variables. Recently, Makri and co-workers [16,17] implemented this idea to path integral calculations of system-bath problems with impressive success. As for the previous case, one can use standard one-dimensional propagation algorithms to evaluate Eq. (2.18). However, speed is of essential importance for the QA scheme, as the propagation algorithm will have to be repeated for each particular value of the system coordinate x . In our calculations the numerical procedure was the following. The system propagator $\langle x | e^{-tH_r} | x_0 \rangle$ was evaluated on a grid of M points $\{x_1, \dots, x_M\}$ by a basis set method. The propagators $\langle \mathbf{z} | e^{-tH_d(x_m)} | \mathbf{y} \rangle$ were then obtained from diagonalization of the coupled bath Hamiltonian $H_d(x_m)$ at each grid value of the system coordinate $\{x_1, \dots, x_M\}$. This is computationally feasible because the bath is assumed to be separable,

$$\langle \mathbf{z} | e^{-tH_d(x_m)} | \mathbf{y} \rangle = \prod_{i=1}^n \langle z_i | e^{-tH_i(x_m)} | y_i \rangle, \quad (2.19)$$

and, therefore, standard one-dimensional algorithms can be used to calculate each factor on the right-hand side of Eq. (2.19). High efficiency was achieved by using a high order finite-difference basis set method described earlier [22].

It is clear that the system-specific propagators [Eqs. (2.14) and (2.18)] are much more difficult to implement than the free-particle representation [Eq. (2.12)]. By construction, however, these are exact for any value of the time increment in the limit where the coupling is turned off. Thus one may expect that they will be accurate for fairly long times with moderate coupling strengths.

Before closing this section three remarks are in order. First, we note that aside from path integral methods [16,17], the idea of employing a good representation as the zeroth-order description of a problem is widely used in perturbation theory [23] and grid and basis set calculations [22,24–26]. Second, the above system-specific propagators can be further improved by using, instead of the Trotter product formula (2.10), higher-order symmetric decompositions. The latter

can easily be constructed by repeated application of the Trotter breakup to give a multisplit factorization of the form [11]

$$e^{-t(H_r+H_d)} = \prod_{i=1} e^{-a_i t H_d} e^{-b_i t H_r} + O(t^{2k+1}). \quad (2.20)$$

The coefficients (a_i, b_i) and the number of operators appearing on the right-hand side of Eq. (2.20) are determined by the desired order of accuracy k . For $k > 1$, one application of Eq. (2.20) requires more computational effort than one application of Eq. (2.10). However, the higher-order decomposition is expected to be more accurate, so that it should allow larger time increments to be taken than the Trotter breakup for comparable accuracy. For some choices, these larger time increments can compensate for the additional computational effort of the higher-order procedure. Although a number of calculations of the real-time properties of quantum systems have been performed using multisplit factorizations [11], the approach has found no application in quantum statistics and nonequilibrium statistical mechanics. The reason is that, beyond second order, any factorization of the form (2.20) must produce some negative coefficients in the set (a_i, b_i) . When applied to Fokker-Planck and/or Bloch equations, this means that negative times must appear at some diffusion operators, making the resulting factorization unbounded. An alternative approach was developed by Drozdov and co-workers [13,14,21], who suggested employing a high-order factorization of the evolution operator, which explicitly includes the commutator of H_r and H_d . This factorization is applicable to many-body problems of both quantum [14] and statistical mechanics [13], allows for the use of improved zeroth-order representations [21], and still requires much less computational effort than multisplit decompositions of Eq. (2.20). Finally, it may be noted that though most of the split operator methods available in the literature are based on symmetric decompositions of the evolution operator, asymmetric factorizations can also be used. We mention specifically the work by Schwartz [27], who developed a simple and efficient method to evaluate low-order nonadiabatic corrections to adiabatic evolution operators. The method is based on an asymmetric product formula derived by Schwartz in terms of his resummation operator technique. As given, though, this formula applies only to calculation of the real-time quantum dynamics of system-bath problems.

B. Power series expansion method

As we already noted, second-order system-specific propagators obtained by a combination of analytic and numerical techniques, though more accurate than the standard Trotter splitting, require significant computational effort if the dimensionality of the system is large. Yet another disadvantage is that with this technique it is rather difficult to go beyond the second order of approximation. Any high-order decomposition, when combined with anharmonic reference systems [like those of Eqs. (2.13) and (2.17)], demands much more computational effort than Trotter-approximated propagators [Eq. (2.10)], and is thus unsuitable for treating truly multidimensional problems. For this reason there has long been a desire to work out a simple computational tool for generating analytic approximations for the propagator accurate for as

long a time increment t as possible and also capable of extension to higher orders of approximation. Only very recently has such a theory been developed in terms of an exponential power series expansion formalism [18,19]. The theory differs from other perturbation techniques [8,23] in that the time evolution operator is approximated by a global polynomial expansion valid not only for short times, but also in the intermediate and long time domains. This is achieved by representing the full propagator as a product of a prescribed zeroth-order propagator P_r with the configuration function

$$P(\mathbf{x}, t | \mathbf{x}^0) = P_r(\mathbf{x}, t | \mathbf{x}^0) \exp[W(\mathbf{x}, \mathbf{x}^0; t)], \quad (2.21)$$

and expanding the exponent of the configuration function in a power series in a given function of t :

$$W(\mathbf{x}, \mathbf{x}^0; t) = \tau^m(t) W_m(\mathbf{x}, \mathbf{x}^0), \quad m \geq 0. \quad (2.22)$$

To be specific, we choose the harmonic-oscillator reference propagator

$$\begin{aligned} P_r(\mathbf{x}, t | \mathbf{x}^0) = & \{ [2\pi \sinh(\omega t) / \omega]^n \det \mathbf{D} \}^{-1/2} \\ & \times \exp \left\{ -\gamma t + \frac{\omega}{2 \sinh(\omega t)} D^{ij} \right. \\ & \left. \times [2x_i x_j^0 - (x_i x_j + x_i^0 x_j^0) \cosh(\omega t)] \right\} \end{aligned} \quad (2.23)$$

and the function $\tau(t)$ given by the width of P_r ,

$$\tau(t) = (1 - e^{-2\omega t}) / 2\omega, \quad (2.24)$$

though a generalization to any but analytic zeroth-order propagator and/or an arbitrary dependence τ of t is also possible [19]. In the above, ω and γ are free parameters to be specified so that the convergence of the series in Eq. (2.22) is as fast as possible [18,19].

The expansion coefficients W_m are determined by inserting Eqs. (2.21) and (2.22) into Eq. (2.1), and equating like powers of τ . This yields, for W_0 ,

$$W_0(\mathbf{x}, \mathbf{x}^0) = \frac{1}{2} [U(\mathbf{x}^0) - U(\mathbf{x})] \quad (2.25)$$

with $U(\mathbf{x})$ given by Eq. (2.2). The rest of the expansion coefficients are expressible in terms of the prescribed function $\varphi(\mathbf{x})$

$$\varphi(\mathbf{x}) = V(\mathbf{x}) - \frac{1}{2} \omega^2 \mathbf{x} \cdot \mathbf{D}^{-1} \mathbf{x} - \gamma. \quad (2.26)$$

These are obtained from a recurrence relation whose explicit form can be found in Ref. [18]. Here we only present the first two expansion coefficients

$$\begin{aligned} W_1 = & - \int_0^1 du \varphi(\mathbf{x}^0 + u \Delta \mathbf{x}), \\ W_2 = & \omega W_1 - \frac{1}{2} \int_0^1 du (1-u) u D_{ij} \partial_{ij}^2 \varphi(\mathbf{q}) |_{\mathbf{q}=\mathbf{x}^0+u\Delta\mathbf{x}}, \end{aligned} \quad (2.27)$$

where $\Delta \mathbf{x} = \mathbf{x} - \mathbf{x}^0$. Since our applications in Sec. III are all covered by a sixth-order polynomial potential

$$V = v_0 + a_i x_i + b_{ij} x_i x_j + c_{ijk} x_i x_j x_k + d_{ijklm} x_i x_j x_k x_l x_m + e_{ijkmp} x_i x_j x_k x_l x_m x_p + f_{ijkmpl} x_i x_j x_k x_l x_m x_p x_l, \quad (2.28)$$

we also present the explicit form taken by Eq. (2.27) in this case:

$$\begin{aligned} W_1 = & -\varphi(\mathbf{x}^0) - \frac{1}{2} a_i \Delta x_i - (b_{ij} - \frac{1}{2} \omega^2 D^{ij})(x_i^0 + \frac{1}{3} \Delta x_i) \Delta x_j - c_{ijk} (\frac{1}{2} \{x^0 x^0 \Delta x\}_{ijk} + \frac{1}{3} \{x^0 \Delta x \Delta x\}_{ijk} + \frac{1}{4} \Delta x_i \Delta x_j \Delta x_k) \\ & - d_{ijklm} (\frac{1}{2} \{x^0 x^0 x^0 \Delta x\}_{ijklm} + \frac{1}{3} \{x^0 x^0 \Delta x \Delta x\}_{ijklm} + \frac{1}{4} \{x^0 \Delta x \Delta x \Delta x\}_{ijklm} + \frac{1}{5} \Delta x_i \Delta x_j \Delta x_k \Delta x_l \Delta x_m), \\ & - e_{ijkmp} (\frac{1}{2} \{x^0 x^0 x^0 x^0 \Delta x\}_{ijkmp} + \frac{1}{3} \{x^0 x^0 x^0 \Delta x \Delta x\}_{ijkmp} + \frac{1}{4} \{x^0 x^0 \Delta x \Delta x \Delta x\}_{ijkmp} + \frac{1}{5} \{x^0 \Delta x \Delta x \Delta x \Delta x\}_{ijkmp} \\ & + \frac{1}{6} \Delta x_i \Delta x_j \Delta x_k \Delta x_l \Delta x_m \Delta x_p) - f_{ijkmpl} (\frac{1}{2} \{x^0 x^0 x^0 x^0 \Delta x\}_{ijkmpl} + \frac{1}{3} \{x^0 x^0 x^0 \Delta x \Delta x\}_{ijkmpl} + \frac{1}{4} \{x^0 x^0 \Delta x \Delta x \Delta x\}_{ijkmpl} \\ & + \frac{1}{5} \{x^0 \Delta x \Delta x \Delta x \Delta x\}_{ijkmpl} + \frac{1}{6} \{x^0 \Delta x \Delta x \Delta x \Delta x \Delta x\}_{ijkmpl} + \frac{1}{7} \Delta x_i \Delta x_j \Delta x_k \Delta x_l \Delta x_m \Delta x_p \Delta x_l), \\ W_2 = & \frac{1}{12} n \omega^2 + \omega W_1 - \frac{1}{12} D_{ij} [2b_{ij} + \{c \dots\}_{ijk} (x_k^0 + \frac{1}{2} \Delta x_k) + \{d \dots\}_{ijklm} (x_k^0 x_l^0 + \frac{1}{2} x_k^0 \Delta x_m + \frac{1}{2} x_m^0 \Delta x_k + \frac{3}{10} \Delta x_k \Delta x_m) \\ & + \{e \dots\}_{ijkmp} (x_k^0 x_m^0 x_p^0 + \frac{1}{2} \{x^0 x^0 \Delta x\}_{kmp} + \frac{3}{10} \{x^0 \Delta x \Delta x\}_{kmp} + \frac{1}{5} \Delta x_k \Delta x_m \Delta x_p) + \{f \dots\}_{ijkmpl} (x_k^0 x_m^0 x_p^0 x_l^0 \\ & + \frac{1}{2} \{x^0 x^0 x^0 \Delta x\}_{kmpl} + \frac{3}{10} \{x^0 x^0 \Delta x \Delta x\}_{kmpl} + \frac{1}{5} \{x^0 \Delta x \Delta x \Delta x\}_{kmpl} + \frac{1}{7} \Delta x_k \Delta x_m \Delta x_p \Delta x_l)], \end{aligned} \quad (2.29)$$

where the curly brackets denote complete symmetrization, i.e.,

$$\{c \dots\}_{ijk} = c_{ijk} + c_{ikj} + c_{kij} + c_{jik} + c_{jki} + c_{kji}. \quad (2.30)$$

The generalization to higher-order polynomials is straightforward.

Ideally, the power series representation of the propagator does not depend on the choice of the free parameters ω and γ . However, as we cannot determine and sum infinitely many terms of the series in Eq. (2.22), we have to truncate it at some finite $m = M$. In this paper we restrict our consideration to $M = 2$ to be consistent with the second-order approximations of the split operator method. Obviously, the accuracy of the truncated power series representation $P_M(\mathbf{x}, t | \mathbf{x}^0)$ is sensitive to ω and γ . The standard way to fix these parameters is to determine them variationally, so that the approximate propagator P_M is accurate for as long a time increment t as possible. It may be noted that the variational approach based on the harmonic-oscillator reference system is of common use in path integral methods [1,15,28], basis set calculations [22] and perturbation theory [29]; consequently, a number of criteria for determining the free parameters have resulted.

In the present calculations we have employed a criterion suggested in Ref. [18]. According to this criterion, the frequency ω is obtained from

$$\frac{1}{2} \omega^2 = \frac{\langle V D^{ij} x_i x_j \rangle_r - \langle V \rangle_r \langle D^{ij} x_i x_j \rangle_r}{\langle (D^{ij} x_i x_j)^2 \rangle_r - \langle D^{ij} x_i x_j \rangle_r^2}, \quad (2.31)$$

where $\langle \dots \rangle_r$ means averaging over the stationary reference probability distribution, i.e.,

$$\langle V \rangle_r = [(\pi/\omega)^n \det \mathbf{D}]^{-1/2} \int d\mathbf{x} V(\mathbf{x}) \exp(-\omega \mathbf{x} \cdot \mathbf{D}^{-1} \mathbf{x}). \quad (2.32)$$

Since the distribution contains the unknown parameter ω , Eq. (2.31) constitutes a self-consistent integral equation. The above criterion is particularly simple to apply to systems with polynomial coefficients, in which case all the integrals in Eq. (2.31) are doable analytically. When applied to Eq. (2.28), this leads to the relation

$$\begin{aligned} 2n\omega^4 - 4\omega^2 D_{ij} b_{ij} - 4\omega \{D \dots D \dots\}_{ijklm} d_{ijklm} \\ - 3\{D \dots D \dots D \dots\}_{ijkmpl} f_{ijkmpl} = 0, \end{aligned} \quad (2.33)$$

which can be readily solved for ω by any root finding procedure.

Next the parameter γ is determined from the normalization condition. For $\Phi(\mathbf{x}) = 0$ (when the purely Fokker-Planck dynamics is concerned), the condition reads

$$\int d\mathbf{x} P(\mathbf{x}, t | \mathbf{x}^0) = 1, \quad (2.34)$$

leading us to

$$\gamma = -(t - \tau - \omega \tau^2)^{-1} \ln \left\{ \int d\mathbf{x} P_2(\mathbf{x}, t | \mathbf{x}^0) \Big|_{\gamma=0} \right\}, \quad (2.35)$$

which is to be evaluated at each time moment of interest. Otherwise, γ is given by

$$\begin{aligned} \gamma = & -\frac{4}{3} \omega \ln \left\{ [(\pi/\omega)^n \det \mathbf{D}]^{-1/2} \right. \\ & \times \int d\mathbf{x} \exp[-\frac{5}{8} \omega D^{ij} x_i x_j - \frac{3}{4} \omega^{-1} V(\mathbf{x}) \\ & \left. - \frac{1}{48} \omega^{-2} D_{ij} \partial_{ij}^2 V(\mathbf{x}) \right\}. \end{aligned} \quad (2.36)$$

which is time independent and is to be evaluated one time in the beginning of calculations. The power series approach outlined above possesses several advantages which deserve to be pointed out.

(i) The recursive evaluation of the propagator is fairly straightforward, and can be readily carried out systematically to any desired order in $\tau(t)$.

(ii) It is a method that can be applied to simple or complex systems, and high dimensionality *does not* present special problems. In many practical applications the potentials $U(\mathbf{x})$ and $\Phi(\mathbf{x})$ are polynomials. In such a case, the function $\varphi(\mathbf{x})$ [Eq. (2.26)] is also a polynomial, and therefore the integrals entering the expansion coefficients are easily evaluated *analytically* for any number of degrees of freedom involved. This is true *regardless* of whether the Hamiltonian allows adiabatic separation of variables [see, e.g., Eqs. (2.13) or (2.17)].

(iii) Having the power series expansion for the propagator permits one to incorporate the true long time limit solution of the problem under study properly, whenever that is known exactly. The latter is a generic case for the purely Fokker-Planck dynamics $\Phi(\mathbf{x})=0$, whose stationary solution is given by Eq. (2.3). A global approximation for the propagator can be obtained by truncating the series in Eq. (2.22) at a given $m=M$, and multiplying the resulting approximation P_M by a correction function F

$$P_g(\mathbf{x},t|\mathbf{x}^0)=F(\mathbf{x},\mathbf{x}^0;t)P_M(\mathbf{x},t|\mathbf{x}^0), \quad (2.37)$$

such that

$$\begin{aligned} F(\mathbf{x},\mathbf{x}^0;t \rightarrow 0) &= 1 + O(\tau^k), \quad k \geq M+1, \\ F(\mathbf{x},\mathbf{x}^0;t \rightarrow \infty) &= P_{st}(\mathbf{x})/P_M(\mathbf{x},t \rightarrow \infty|\mathbf{x}^0). \end{aligned} \quad (2.38)$$

In a simplest realization, this gives

$$\begin{aligned} P_g(\mathbf{x},t|\mathbf{x}^0) &= P_M(\mathbf{x},t|\mathbf{x}^0) \exp\{(2\omega\tau)^{M+1} \\ &\quad \times \ln[P_{st}(\mathbf{x})/P_M(\mathbf{x},t \rightarrow \infty|\mathbf{x}^0)]\}. \end{aligned} \quad (2.39)$$

III. APPLICATIONS

In this section we give three examples illustrating the efficiency and accuracy of the various second-order approximations for the *single-step propagator* discussed in Sec. II. The examples selected involve only two degrees of freedom so that exact results and quadiabatic approximations can be generated in a reasonable amount of time. The former are obtained using a high-order split-operator fast Fourier trans-

form method [14]. While the integral appearing in the quadiabatic propagator [Eq. (2.18)] is evaluated by matrix multiplication.

A. System-bath Hamiltonian

To begin with, we consider the generic system-bath Hamiltonian

$$H = -\frac{1}{2}D_x\partial_{xx}^2 + V(x) - \frac{1}{2}D_y\partial_{yy}^2 + (\Omega^2/2D_y)(y - \lambda x)^2, \quad (3.1)$$

which gives rise to one of the simplest and most intensively studied models of dynamical processes in the condensed phase. The model involves a relevant coordinate x (describing the nonlinear system of interest) coupled to a harmonic ‘‘bath’’ degree of freedom y that mimics the effect of the environment, with λ being the coupling parameter. A great deal of effort has been devoted in recent times to the construction of rigorous numerical or approximate analytical methods for efficiently treating system-bath Hamiltonians [14,16,17,21,25,27].

To be specific, we choose the system potential to be a pure quartic oscillator

$$V(x) = \frac{1}{4}x^4. \quad (3.2)$$

Following the SA scheme, we take H_r as the entire separable part of the full Hamiltonian

$$\begin{aligned} H_r &= -\frac{1}{2}D_x\partial_{xx}^2 + V(x) + (\lambda^2\Omega^2/2D_y)x^2 \\ &\quad - \frac{1}{2}D_y\partial_{yy}^2 + (\Omega^2/2D_y)y^2, \\ F &= -(\lambda\Omega^2/D_y)xy. \end{aligned} \quad (3.3)$$

Moreover, in order to exploit the adiabatic reference (the QA scheme), we partition Eq. (3.1) into a Hamiltonian for the system and an adiabatically displaced harmonic-oscillator Hamiltonian reading

$$\begin{aligned} H_r &= -\frac{1}{2}D_x\partial_{xx}^2 + V(x), \\ H_d &= -\frac{1}{2}D_y\partial_{yy}^2 + (\Omega^2/2D_y)(y - \lambda x)^2. \end{aligned} \quad (3.4)$$

Since the bath Hamiltonian H_d depends only parametrically on the system coordinate, the corresponding matrix element is easily obtained analytically. It is nothing but the propagator of a shifted harmonic oscillator. Taking advantage of the fact that this propagator is Gaussian in y , Eq. (2.18) takes the form

$$\begin{aligned} \psi_{qa}(x,y,t|x_0,y_0) &= \langle x|e^{-tH_r}|x_0\rangle \sqrt{\frac{\Omega}{2\pi D_y \sinh \Omega t}} \exp\frac{\Omega}{2D_y \sinh \Omega t} \{2(y - \lambda x)(y_0 - \lambda x_0) - \lambda(x - x_0) \\ &\quad \times \cosh^2 \frac{1}{2}\Omega t - 2\lambda(x - x_0)(y - y_0 + \lambda x_0 - \lambda x) \cosh \frac{1}{2}\Omega t - [(y - \lambda x)^2 + (y_0 - \lambda x_0)^2] \cosh \Omega t\}. \end{aligned} \quad (3.5)$$

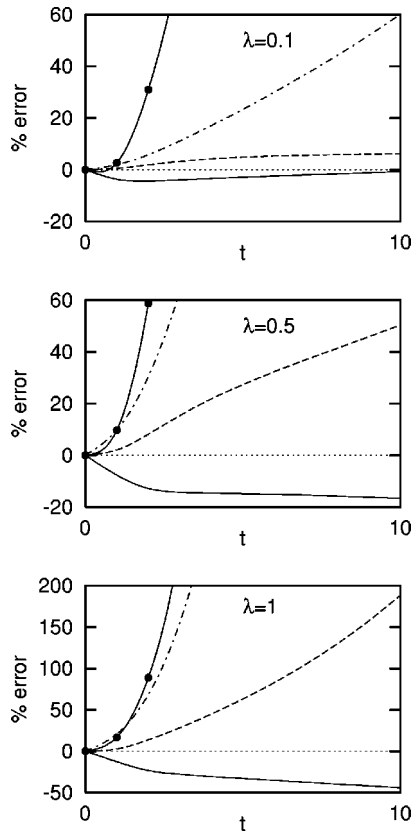


FIG. 1. Percentage error in the off-diagonal matrix element [Eq. (3.6)] of the system-bath Hamiltonian [Eqs. (3.1) and (3.2)] for $\lambda = 0.1, 0.5,$ and 1 . Circles connected by solid lines, standard Trotter splitting [Eq. (2.12)]; dot-dashed lines, SA scheme [Eqs. (2.14) and (3.3)]; dashed lines, quasiadiabatic propagator [Eq. (3.5)]; solid lines, second-order power series expansion [Eqs. (2.21) and (2.22)].

We would like to emphasize that it is just this kind of Hamiltonian for which the quasiadiabatic representation of the propagator was designed [16,22,25,27]). Only very recently, Makri and co-workers [16] applied Eq. (3.5) to path integral calculations of chemical dynamics with impressive success. Furthermore, the generalization of Eq. (3.5) to an arbitrary number of bath degrees of freedom is straightforward and does not complicate the final expression [16]. It is in this particular case that implementing the quasiadiabatic propagator numerically is not more difficult than in the SA scheme. Both schemes are exact when the coupling is turned off. One may thus expect that they would be accurate for systems with moderate coupling. As far as the power series expansion method is concerned, the above model is challenging for it not only when the coupling is strong but also in the separable limit. This is because the Hamiltonian remains highly anharmonic even though $\lambda = 0$.

The accuracy of the various approximations for the propagator is investigated by calculating the off-diagonal matrix element

$$\langle x, y | e^{-tH} | x_0, y_0 \rangle \quad \text{with} \quad x = y = 1 \quad \text{and} \quad x_0 = y_0 = 0. \quad (3.6)$$

The calculation is performed at $D_x = D_y = \Omega = 1$ for different values of the coupling parameter λ . The results are presented in Fig. 1. Surprisingly, the power series expansion (although

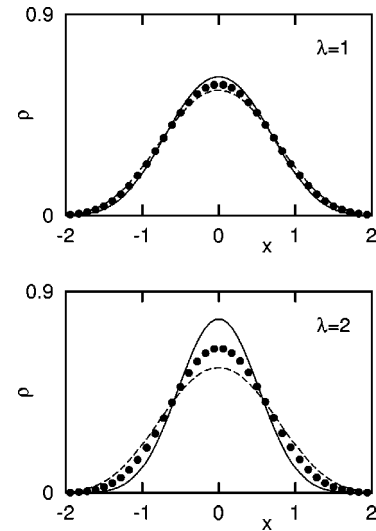


FIG. 2. Probability distribution [as defined in Eq. (3.7)] of the system-bath Hamiltonian [Eqs. (3.1) and (3.2)] obtained for $\lambda = 1$ and 2 . Solid lines, second-order power series expansion; dashed lines, quasiadiabatic propagator; circles, exact numerical results.

it involves no anharmonic reference) works much better than the Trotter-approximated propagators. As evidenced by the figure, it quite accurately describes the dynamics of the system-bath problem in the entire time domain for both weak and moderate coupling. This is in drastic contrast to the quasiadiabatic representation of Makri and co-workers [16], [Eq. (3.5)]. The latter accurately describes the dynamics over a broad range of t only for $\lambda \leq 0.1$. With increasing coupling, however, the accuracy of Eq. (3.5) deteriorates very rapidly, and already for $\lambda \geq 0.3$ it fails to provide correct results. The SA scheme also substantially improves the standard Trotter splitting only if the coupling is weak ($\lambda = 0.1$), while for a stronger coupling it works not better than Eq. (2.12). Finally, in all the cases considered the error made by the the standard Trotter splitting increases with t almost exponentially, and very soon grows out of the scale of the figure.

For completeness, we show in Fig. 2 results obtained for the system probability distribution as t goes to infinity:

$$\rho(x) = \int_{-\infty}^{\infty} dy P(x, y, t \rightarrow \infty). \quad (3.7)$$

However, before discussing the results, three remarks are in order. First, we recall that this function is related to the ground state solution through Eq. (2.8). Second, neither Eq. (2.12) nor (2.14) can be normalized for $\lambda \neq 0$ as $t \rightarrow \infty$. That is why these approximations are not presented in the figure. Third, within the scope of the quasiadiabatic approximation the function $\rho(x)$ is independent of λ and given by

$$\rho(x) = \lim_{t \rightarrow \infty} \langle x | e^{-tH} | x \rangle / \text{Tr}[e^{-tH}], \quad (3.8)$$

which is simply the square of the ground state wave function of the uncoupled system. It is remarkable that the true system probability distribution indeed remains insensitive to the coupling strength over a broad range of λ . As shown by Fig. 2, the deviation of Eq. (3.8) from the numerically exact re-

sults remains small even though $\lambda = 1$. Of course, with further increasing coupling the deviation also increases, but this happens rather slowly.

B. Modified Hénon-Heiles potential

As a second example, we consider a modified (bound) Hénon-Heiles Hamiltonian of the form [30]

$$H = -\frac{1}{2}(\partial_{xx}^2 + \partial_{yy}^2) + \frac{1}{2}(x^2 + y^2) + \lambda x(y^2 - \frac{1}{3}x^2) + \frac{1}{16}\lambda^2(x^2 + y^2)^2, \quad (3.9)$$

where the coupling parameter λ is a measure of anharmonicity. The Hénon-Heiles Hamiltonian [31] is a chaotic model that (classically) describes a resonating system. It has been used as a model for many classical or quantum studies of nonlinear molecular dynamics [32]. The Hénon-Heiles Hamiltonian is also important in numerical analysis. It has frequently been exploited to test the utility of different numerical schemes [4,24,30,33]. In all these investigations, however, the coupling parameter λ was taken to be rather small, $\lambda \sim 0.1$, so that the Hamiltonian was close to the two-dimensional harmonic oscillator. In the present testing, in order for the model to present a challenge for the methods outlined in Sec. II, we carried out calculations over a wide range of coupling strengths, ranging from the harmonic oscillator ($\lambda = 0$) to a very anharmonic process ($\lambda = 2$).

Following the SA scheme, we choose H_r as the separable part of the Hamiltonian

$$H_r = -\frac{1}{2}(\partial_{xx}^2 + \partial_{yy}^2) + \frac{1}{2}(x^2 + y^2) - \frac{1}{3}\lambda x^3 + \frac{1}{16}\lambda^2(x^4 + y^4); \quad (3.10)$$

accordingly,

$$F = \lambda xy^2 + \frac{1}{8}\lambda^2 x^2 y^2. \quad (3.11)$$

On the other hand, to calculate the propagator within the scope of the QA scheme, we split Eq. (3.9) into a system Hamiltonian H_r and an anharmonic bath H_d reading

$$H_r = -\frac{1}{2}\partial_{xx}^2 + \frac{1}{2}x^2 - \frac{1}{3}\lambda x^3 + \frac{1}{16}\lambda^2 x^4, \quad (3.12)$$

$$H_d = -\frac{1}{2}\partial_{yy}^2 + \frac{1}{2}y^2 + \lambda xy^2 + \frac{1}{16}\lambda^2(y^4 + 2x^2 y^2).$$

It should be pointed out that the Hénon-Heiles Hamiltonian is anharmonic in both variables. As a result, the numerical implementation of the quasiadiabatic propagator, Eqs. (2.18) and (3.12), is not as simple as in the case of the system-bath Hamiltonian considered Sec. III A [cf. Eq. (3.5)]. It is enough to say that the necessary computational effort is much larger than that of the standard grid propagation scheme used to generate numerically exact results. With increasing dimensionality, however, the situation becomes better. In such a case, the numerical work in the standard scheme grows exponentially, while the quasiadiabatic approximation requires a computational effort that scales only linearly with the number of degrees of freedom involved.

In order to understand how dependent the accuracy of the various approximations for the propagator is on the coupling

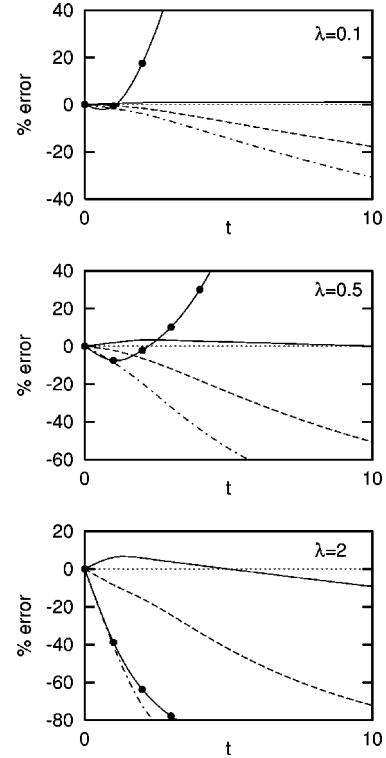


FIG. 3. Same as Fig. 1 but for the modified Hénon-Heiles Hamiltonian [Eq. (3.9)] with $\lambda = 0.1, 0.5,$ and 2 . The SA [Eq. (2.14)] and QA [Eq. (2.18)] propagators are calculated by partitioning the Hamiltonian according to Eqs. (3.10) and (3.12), respectively.

strength, we again calculated the off-diagonal matrix element and the probability distribution as defined by Eqs. (3.6) and (3.7), respectively. Figure 3 shows the relative error in the off-diagonal matrix element obtained for $\lambda = 0.1, 0.5,$ and 2 . As anticipated, the standard Trotter splitting [Eq. (2.12)] gives the worst approximation of the exact results. The error made by this propagator increases with t very rapidly, and for $t = 10$ it overestimates the matrix element by several orders of magnitude. This is the case regardless of the particular value of the coupling parameter λ . Use of the improved zeroth-order representations [Eqs. (3.10) and (3.12)] is seen to reduce the error of the Trotter breakup considerably, provided the coupling is weak enough ($\lambda = 0.1$). Even in that case, however, the utility of the system-specific propagators is restricted to the intermediate time domain. As the coupling strength increases, the range of applicability of the Trotter-approximated propagators rapidly decreases, and for $\lambda = 0.5$ these are all valid only for short times. The power series expansion is in very good agreement with the numerically exact results in the weak coupling limit. The agreement becomes worse with increasing coupling but rather slowly, so that even for $\lambda = 2$ the method still provides an accurate description over a broad range of t . The results presented demonstrate the potential of the power series approach. It is seen to be able to describe correctly the dynamics of a very anharmonic process for fairly long times. For comparison, the improved Trotter-approximated propagators provide a level of accuracy comparable with that of the power series expansion method only for $\lambda \leq 0.01$, when the Hamiltonian is very close to the two-dimensional harmonic oscillator.

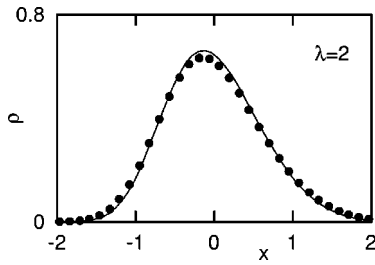


FIG. 4. Same as in Fig. 2, but for the modified Hénon-Heiles Hamiltonian [Eq. (3.9)] with $\lambda=2$.

It is also remarkable that the efficiency of the power series expansion method in giving precise ground state solutions appears to be rather insensitive to the coupling strength. As illustrated in Fig. 4, it works equally well for both moderate and large coupling strengths, to say nothing about the weak coupling limit. The same is not true for the Trotter-approximated propagators, none of which can be normalized as t goes to infinity, excepting the trivial case $\lambda=0$.

C. Fokker-Planck chaotic system

As a third more sophisticated example, selected to illustrate the use of the present methods, we consider the stochastic dynamics in a two-dimensional potential with strongly anharmonic mode coupling. The model is governed by the Fokker-Planck equation

$$\begin{aligned} \partial_t P(x,y,t|x_0,y_0) = & [\partial_x(\partial_x U) + \partial_y(\partial_y U) + \frac{1}{2}D(\partial_{xx}^2 + \partial_{yy}^2)] \\ & \times P(x,y,t|x_0,y_0), \end{aligned} \quad (3.13)$$

$$U = 2x^4 + \frac{3}{5}y^4 + \lambda xy(x-y)^2,$$

whose stationary solution is known to be

$$P_{\text{st}}(x,y) = N^{-1} \exp[-2U(x,y)/D]. \quad (3.14)$$

It will be recalled that the normalization constant N is determined from Eq. (2.34). Transformation (2.4) casts the above equation into a Hermitian Schrödinger-type form with the Hamiltonian

$$H = -\frac{1}{2}D(\partial_{xx}^2 + \partial_{yy}^2) + \Phi, \quad (3.15)$$

$$\begin{aligned} \Phi = \frac{1}{2D} \{ & (64 + \lambda^2)x^6 + \lambda[(48 - 8\lambda)x^5y + (31\lambda - 64)x^4y^2 + (\frac{104}{5} - 48\lambda)x^3y^3 + (31\lambda - \frac{96}{5})x^2y^4 \\ & + (\frac{72}{5} - 8\lambda)xy^5] + (\frac{144}{25} + \lambda^2)y^6\} - (12 - 2\lambda)x^2 - (\frac{18}{5} - 2\lambda)y^2 - 6\lambda xy. \end{aligned}$$

This model was introduced by Millonas and Reichl [34] when studying stochastic chaos. The latter term was used to describe the observation of chaos in the classical trajectories of the corresponding Hamilton's equations of motion,

$$\dot{p}_i = -\frac{\partial \mathcal{H}}{\partial q_i}, \quad \dot{q}_i = \frac{\partial \mathcal{H}}{\partial p_i}, \quad (3.16)$$

where $\mathbf{q}=(x,y)$, $\mathbf{p}=(p_x,p_y)$, and the Hamiltonian reads

$$\mathcal{H} = \frac{1}{2}\mathbf{p}^2 + D\Phi, \quad (3.17)$$

with the potential $\Phi(x,y)$ given by Eq. (3.15). Millonas and Reichl [34] calculated, for $D=0.2$ and $0 \leq \lambda \leq 0.14$, the eigenvalues of Eq. (3.13) by expanding H in a harmonic-oscillator basis and truncating the matrix at a suitably large size. Taking advantage of the fact that H is parity invariant enabled them to compute the eigenvalues for the even and odd parity matrices separately, using two sets of 2600 basis functions for each parity. Analyzing the spectral properties of Eq. (3.13) as a function of the coupling parameter λ , these authors arrived at the conclusion that the system should exhibit a transition to chaos for $\lambda \geq 0.14$. More recently, Ingber [35] performed an accurate calculation, for $D=0.2$ and $0.1 \leq \lambda \leq 0.55$, of the time evolution of $P(x,y,t|0,0)$ by means of a path integral method, requiring up to 2000 foldings. The main findings revealed in his numerical calculations are the following. The system appears to be very stable with a single peak in its probability up through $\lambda = 0.5$. The onset of instabilities first occurs at $\lambda = 0.55$. However, Ingber failed to establish the reason why the instabilities appear.

Following Ingber, we also calculated the time evolution of $P(x,y,t|0,0)$ at $D=0.2$ for different values of the coupling strength, and compared the numerically exact results with those obtained from the approximate propagators. The improved zeroth-order representations we have used in this case are

$$\begin{aligned} H_r = & -\frac{1}{2}D(\partial_{xx}^2 + \partial_{yy}^2) + \frac{1}{2}D^{-1}[(64 + \lambda^2)x^6 + (\frac{144}{25} + \lambda^2)y^6] - (12 - 2\lambda)x^2 - (\frac{18}{5} - 2\lambda)y^2, \\ H_d = & \lambda xy \{ \frac{1}{2}D^{-1}[(48 - 8\lambda)x^4 + (31\lambda - 64)x^3y + (\frac{104}{5} - 48\lambda)x^2y^2 + (31\lambda - \frac{96}{5})xy^3 + (\frac{72}{5} - 8\lambda)y^4] - 6 \}, \end{aligned} \quad (3.18)$$

and

$$\begin{aligned}
 H_r &= -\frac{1}{2}D\partial_{xx}^2 + \frac{1}{2}D^{-1}(64 + \lambda^2)x^6 - (12 - 2\lambda)x^2, \\
 H_d &= -\frac{1}{2}D\partial_{yy}^2 - (\frac{18}{5} - 2\lambda)y^2 - 6\lambda xy + \frac{1}{2D}\{\lambda[(48 - 8\lambda)x^5y + (31\lambda - 64)x^4y^2 \\
 &\quad + (\frac{104}{5} - 48\lambda)x^3y^3 + (31\lambda - \frac{96}{5})x^2y^4 + (\frac{72}{5} - 8\lambda)xy^5] + (\frac{144}{25} + \lambda^2)y^6\}.
 \end{aligned}
 \tag{3.19}$$

The former is chosen according to the SA scheme [Eqs. (2.13) and (2.14)], while the latter corresponds to adiabatic separation of variables [Eqs. (2.17) and (2.18)]. But before presenting our results we would like to indicate the reason for the cause of appearance of instabilities. It lies in the fact that the stationary solution [Eq. (3.14)] is nontrivial if and only if $|\lambda| < 0.54$. Just in that range of coupling strengths the normalization constant N remains finite. Meanwhile for $|\lambda| \geq 0.54$, the potential $U(x,y)$ is no longer unbounded from above as x and y go to infinity. Consequently, N becomes infinite, and the stationary solution reduces to $P_{st} = 0$. This is well illustrated by Fig. 5, which shows that the contour plot of the basin exhibits a transition as the coupling parameter λ is varied. The contour lines are seen to be closed for $\lambda < 0.54$, whereas at $\lambda = 0.54$ a valley appears along which the potential remains finite with increasing x and y .

Turning back to the discussion of the various approximations for the propagator, we would like to emphasize that the above model presents a particular challenge for the power series approach; it remains highly anharmonic whatever the coupling constant λ is [see Eq. (3.15)]. On the other hand, since the stationary solution of Eq. (3.13) is known exactly, the extrapolation formula (2.39) can be used to construct a global approximation for the propagator. The global approximation is obviously exact in both limits of short and long times for all values of λ from the interval $[0, 0.53]$. Therefore, one may expect that it would be reasonably accurate in the intermediate time domain as well. Moreover, we note that the accuracy of the approximate propagators is investigated through the calculation of the off-diagonal matrix element

$$P(x,y,t|x_0,y_0) \text{ with } x=y=0.15 \text{ and } x_0=y_0=0.
 \tag{3.20}$$

The final point (x,y) in Eq. (3.20) is taken to be close to the

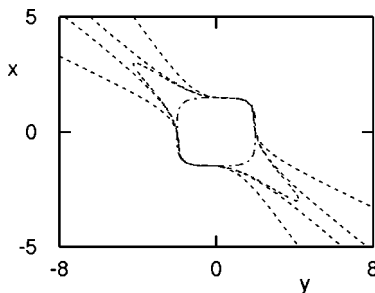


FIG. 5. Contour lines $U(x,y) = 10$ of potential (3.13) for $\lambda = 0, 0.52, 0.54, \text{ and } 0.8$.

origin to keep an acceptable level of accuracy of the SA and QA schemes. Both are found to diverge very rapidly with time as $|x|$ and $|y|$ increase.

The results obtained for the off-diagonal matrix element are presented in Fig. 6. The overall situation is seen to be quite similar to the case of the Hénon-Heiles Hamiltonian. As shown by the figure, the standard short time approximation is least accurate. Use of the quasiadiabatic zeroth-order representation improves the accuracy of the Trotter breakup in the intermediate time domain, but its numerical implementation is more arduous than a conventional numerically exact calculation. The SA scheme works a bit better than the quasiadiabatic propagator, though its validity is also generally restricted to short times and/or small coupling strengths. In contrast, the global power series approximation for the propagator provides an accurate description of the dynamics over a broader range of λ in the *entire* time domain, and still

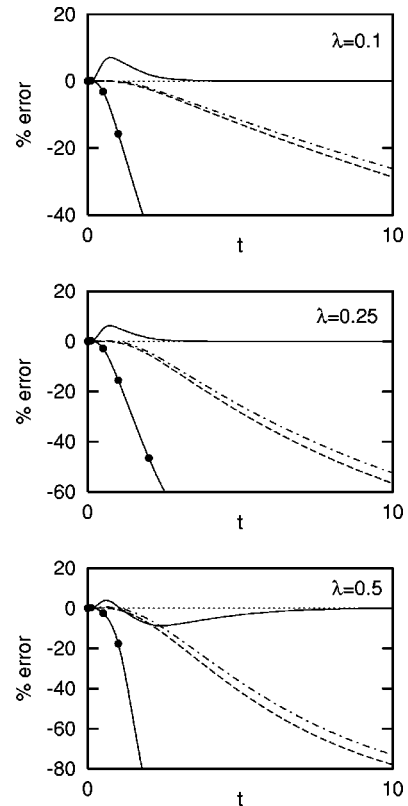


FIG. 6. Same as in Fig. 1, but for the off-diagonal matrix element [Eq. (3.20)] of the stochastic model [Eq. (3.13)] with $D = 0.2$ and $\lambda = 0.1, 0.25, \text{ and } 0.5$. The SA [Eq. (2.14)] and QA [Eq. (2.18)] propagators are calculated by partitioning the Hamiltonian according to Eqs. (3.18) and (3.19), respectively. Solid lines are for the global second-order approximation [Eq. (2.39)].

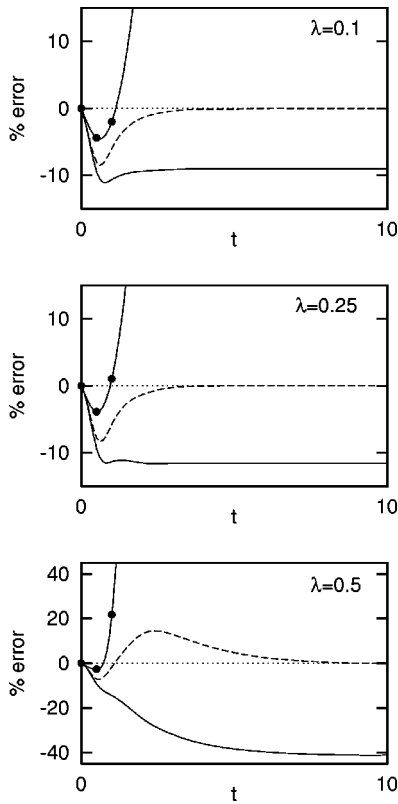


FIG. 7. Percentage error in the second cumulant [Eq. (3.21)] of the stochastic model [Eq. (3.13)]. Circles connected by solid lines, standard short time propagator [Eq. (2.12)]; dashed lines, power series expansion [Eqs. (2.21) and (2.22)]; solid lines, second-order global approximation [Eq. (2.39)].

requires no computational effort.

The relative efficacy of the ordinary and global power series approximations for the propagator is seen from Fig. 7, which shows the relative error in the second cumulant

$$\sigma(t) = \langle x^2(t) \rangle - \langle x(t) \rangle^2, \quad (3.21)$$

where

$$\langle x^n(t) \rangle = \int_{-\infty}^{\infty} dx \int_{-\infty}^{\infty} dy x^n P(x, y, t). \quad (3.22)$$

Also shown are results obtained with the standard Trotter splitting. The corresponding errors of the two system-specific propagators are not presented in the figure, because both fail to provide convergent results for the second cumulant whatever $\lambda \neq 0$. It is clear from Fig. 7 that the range of applicability of the power series expansion method is quite robust to variations in the coupling strength. One would expect the accuracy of Eqs. (2.21) and (2.22) to fall off very quickly as λ goes up, but in fact, going from a potential of $\lambda = 0.1$ to one about $\lambda = 0.5$, there was a slow decay in the accuracy of the results. It is also seen that the use of the interpolating formula (2.39) substantially improves the approach, considerably decreasing the error in the entire time

domain. The error made by the standard Trotter splitting is again very large compared to that of the power series expansion.

IV. CONCLUDING REMARKS

In this paper we have formulated and applied two different approaches to calculating quantum and statistical mechanics of multidimensional nonlinear systems, namely, the split operator method and the power series expansion formalism. Our study was not intended to be an exhaustive comparison of these techniques, but rather intended to illustrate their stability and relative efficacy in giving precise dynamical properties in a simple economic way. Both approaches are perturbative in the coupling potential and the time increment, but the manner in which higher-order corrections can be taken into account (as well as the way in which the potential enters the methods) is quite different. For this reason, the strategy followed made use of the second-order approximations to avoid having to evaluate numerically multidimensional integrals that necessarily arise in high-order split operator decompositions. Similarly, the examples considered are chosen to be two dimensional in order to allow a comparison with a conventional grid method without extraordinary computational effort.

From a vast amount of possibilities, we selected three different rather general ways to partition the underlying Hamiltonian operator that have been frequently used by many researchers. These are (i) the standard splitting of the Hamiltonian into potential and kinetic energy terms, (ii) the SA scheme using the separable part of the Hamiltonian as a zeroth-order representation, and (iii) the quasiadiabatic approximation based on partitioning the Hamiltonian into a one-dimensional system part coupled to a bath of noninteracting degrees of freedom. Although system-specific propagators, by construction, incorporate the exact dynamics of anharmonic zeroth-order representations, this will not always assure us accurate results (e.g., what if the system does not behave adiabatically at all?). The calculations we performed clearly demonstrate that the efficiency of the approach depends crucially on the decision about which part of the Hamiltonian properly describes the dynamics in the intermediate time domain. In some cases, a clear disparity between variables makes the choice obvious. Thus, for instance, the approach works well in the separable limit when the coupling is almost turned off ($\lambda \leq 0.01$). In this case, the system-specific propagators indeed remain correct for times sufficiently long to observe physical effects. Otherwise, choosing the best partitioning of the system is more of an art than an exact science. Still, an improper choice can result in a less than optimally efficient propagator, or even one which is worse than the standard short time propagator.

It is remarkable that in all the cases considered the best agreement with exact numerical calculations was attained with the power series representation of the propagator. The method holds regardless of whether the Hamiltonian allows adiabatic separation of variables. It is capable of accurately describing the dynamics of *very anharmonic processes* in the *entire* time domain. The latter is particularly surprising, as the present power series expansion involves *no* anharmonic

reference system. Yet another appealing feature of the power series approach is the ease with which it can be implemented numerically. The necessary calculations can be performed analytically for *any* number of degrees of freedom, which makes the method very attractive for treating many-body problems. This, however, is in general true only for poly-

mial potentials. For others, its numerical implementation may be very arduous.

ACKNOWLEDGMENT

Financial support from the Ministry of Education, Science, Sports, and Culture of Japan is greatly appreciated.

-
- [1] R. P. Feynman and A. R. Hibbs, *Quantum Mechanics and Path Integrals* (McGraw-Hill, New York, 1965); R. P. Feynman, *Statistical Mechanics* (Benjamin, Reading, MA, 1972). H. Kleinert, *Path Integrals in Quantum Mechanics, Statistical and Polymer Physics* 2nd ed. (World Scientific, Singapore, 1995).
- [2] L. S. Schulman, *Techniques and Applications of Path Integration* (Wiley, New York, 1981); F. Langouche, D. Roekaerts, and Tirapegui, *Functional Integration and Semiclassical Expansions, Mathematics and Its Applications* (Reidel, Dordrecht, 1982); D. C. Khandekar, S. V. Lawande, and K. Bhagwat, *Path Integral Methods and Their Applications* (World Scientific, Singapore, 1993); H. Kleinert, *Path Integrals in Quantum Mechanics, Statistics, and Polymer Physics*, 2nd ed. (World Scientific, Singapore, 1995).
- [3] For a recent review see J. Math. Phys. **36**, 5 (1995), special thematic issue on Functional Integration, edited by C. DeWitt-Morette.
- [4] M. D. Feit, J. A. Fleck, Jr., and A. Steiger, J. Comput. Phys. **47**, 412 (1982).
- [5] N. Metropolis, A. W. Rosenbluth, M. N. Rosenbluth, H. Teller, and E. Teller, J. Chem. Phys. **21**, 1087 (1953); K. Binder and D. W. Heermann, *Monte Carlo Simulation in Statistical Physics* (Springer, Berlin, 1988).
- [6] See, e.g., J. Stat. Phys. **43**, 5/6 (1986). This special issue contains the Proceedings of the Conference on Frontiers of Quantum Monte Carlo, edited by J. E. Gubernatis.
- [7] V. S. Filinov, Nucl. Phys. B **271**, 717 (1986); B. J. Berne and D. Thirumalai, Annu. Rev. Phys. Chem. **37**, 401 (1986); J. D. Doll and D. L. Freeman, Adv. Chem. Phys. **73**, 120 (1988); N. Makri, Comput. Phys. Commun. **63**, 389 (1991); O. A. Sharafeddin, D. J. Kouri, N. Nayar, and D. K. Hoffman, J. Chem. Phys. **95**, 3224 (1991); D. J. Kouri, W. Zhu, X. Ma, B. M. Pettitt, and D. K. Hoffman, J. Phys. Chem. **96**, 9622 (1992); T. L. Marchioro II, M. Arnold, D. K. Hoffman, W. Zhu, Y. Huang, and D. J. Kouri, Phys. Rev. E **50**, 2320 (1994).
- [8] N. Makri and W. H. Miller, J. Chem. Phys. **90**, 904 (1989); A. N. Drozdov, Physica A **196**, 283 (1993).
- [9] K. E. Schmidt and M. A. Lee, Phys. Rev. E **51**, 5495 (1995); A. N. Drozdov, J. Chem. Phys. **107**, 3505 (1997).
- [10] A. N. Drozdov, Phys. Rev. E **55**, 2496 (1997).
- [11] A. D. Bandrauk and H. Shen, Chem. Phys. Lett. **176**, 428 (1991); M. Glasner, D. Yevick, and B. Hermansson, J. Chem. Phys. **95**, 8266 (1991); M. Suzuki, J. Math. Phys. **32**, 400 (1991).
- [12] H. De Raedt and B. De Raedt, Phys. Rev. A **28**, 3575 (1983); S. A. Chin, Phys. Lett. A **226**, 344 (1997).
- [13] A. N. Drozdov and J. J. Brey, Phys. Rev. E **57**, 1284 (1998); A. N. Drozdov and P. Talkner, J. Chem. Phys. **109**, 2080 (1998).
- [14] A. N. Drozdov, J. Chem. Phys. **108**, 6580 (1998).
- [15] A. N. Drozdov and J. J. Brey, Phys. Rev. E **57**, 146 (1998).
- [16] M. Topaler and N. Makri, J. Chem. Phys. **97**, 9001 (1992); **101**, 7500 (1994); D. Makarov and N. Makri, Phys. Rev. A **48**, 3626 (1994); N. Makri, J. Math. Phys. **35**, 2430 (1995).
- [17] G. Ilk and N. Makri, J. Chem. Phys. **101**, 6708 (1994).
- [18] A. N. Drozdov, J. Chem. Phys. **105**, 515 (1996).
- [19] A. N. Drozdov, Phys. Rev. E **55**, 1496 (1997).
- [20] C. W. Gardiner, *Handbook of Stochastic Methods* (Springer, Berlin, 1983); H. Risken, *The Fokker-Planck Equation, Methods of Solution and Applications*, 2nd ed. (Springer, New York, 1989).
- [21] A. N. Drozdov and J. J. Brey, Phys. Rev. E **58**, 2859 (1998).
- [22] A. N. Drozdov and P. Talkner, J. Chem. Phys. **105**, 4117 (1996).
- [23] R. A. Corns, J. Phys. A **27**, 593 (1994); M. Roncadelli, Phys. Rev. E **52**, 4661 (1995).
- [24] B. Shizgal and H. Chen, J. Chem. Phys. **104**, 4137 (1996).
- [25] N. Makri and W. H. Miller, J. Chem. Phys. **86**, 1451 (1987); A. N. Drozdov and P. Talkner, Phys. Rev. E **54**, 6160 (1996).
- [26] S. Das and D. J. Tannor, J. Chem. Phys. **92**, 3403 (1990); C. J. Williams, J. Qian, and D. J. Tannor, *ibid.* **95**, 1721 (1991).
- [27] S. D. Schwartz, J. Chem. Phys. **104**, 1394 (1996); **105**, 6871 (1996); **107**, 2424 (1997); **108**, 3620 (1998).
- [28] R. Giachetti and V. Tognetti, Phys. Rev. Lett. **55**, 912 (1986); G. A. Voth, D. Chandler, and W. H. Miller, J. Chem. Phys. **91**, 7749 (1989); J. Cao and B. J. Berne, *ibid.* **92**, 7531 (1990).
- [29] G. A. Arteca, F. M. Fernández, and E. A. Castro, *Large Order Perturbation Theory and Summation Methods in Quantum Mechanics* (Springer-Verlag, Berlin, 1990); W. Janke and H. Kleinert, Phys. Rev. Lett. **75**, 2787 (1995); E. J. Weniger, *ibid.* **77**, 2859 (1996).
- [30] H.-D. Meyer, U. Manthe, and L. S. Cederbaum, Chem. Phys. Lett. **165**, 73 (1990); E. Sim and N. Makri, J. Chem. Phys. **102**, 5616 (1995).
- [31] M. Hénon and C. Heiles, Astron. J. **69**, 73 (1964); G. H. Walker and J. Ford, Phys. Rev. **188**, 416 (1969).
- [32] See, e.g., M. C. Gutzwiller, *Chaos in Classical and Quantum Mechanics* (Springer, New York, 1990); A. J. Lichtenberg and M. A. Leiberman, *Regular and Chaotic Dynamics* (Springer, New York, 1991).
- [33] D. W. Noid and R. A. Marcus, J. Chem. Phys. **62**, 2119 (1975); D. W. Noid, M. L. Koszykowski, M. Tabor, and R. A. Marcus, *ibid.* **72**, 6169 (1980); M. J. Davis and E. J. Heller, *ibid.* **71**, 3383 (1979); R. Kosloff and H. Tal-Ezer, Chem. Phys. Lett. **127**, 223 (1986); G. C. Groenboom and H. M. Buck, J. Chem. Phys. **92**, 4374 (1990); D. S. Zhang, G. W. Wei, D. J. Kouri, and D. K. Hoffman, *ibid.* **106**, 5216 (1997).
- [34] M. M. Millonas and L. E. Reichl, Phys. Rev. Lett. **68**, 3125 (1992).
- [35] L. Ingber, Phys. Rev. E **51**, 1616 (1995).